

10-Gb/s Agile Wavelength Conversion With Nanosecond Tuning Times Using a Multisection Widely Tunable Laser

Olga A. Lavrova, Lavanya Rau, *Student Member, IEEE*, and Daniel J. Blumenthal, *Senior Member, IEEE, Member, OSA*

Abstract—Simultaneous wavelength conversion and high-speed wavelength switching has been demonstrated using a multisection grating-assisted coupled sampled reflector laser. A high-output extinction ratio (> 20 dBm) over a 30-nm wavelength range was observed. The 10-Gb/s data was switched between different output wavelengths at a 2.5-Gb/s rate and transmitted over 50 km of dispersion-shifted fiber with a small measured power penalty (< 2 dB).

Index Terms—Optoelectronic devices, semiconductor lasers, tunable circuits and devices, wavelength division multiplexing (WDM).

I. INTRODUCTION

WAVELENGTH conversion (WC) is a key function of future all-optical networks and can be used to dynamically route signals, regenerate data, avoid wavelength blocking, and ease wavelength management. New optical packet switching applications will require agile wavelength converters that can route individual packets by tuning to a new output wavelength within nanoseconds [1].

The two key subfunctions for agile applications are the optically controlled wavelength converter and the fast tunable wavelength source. Wavelength converters that employ active semiconductor gain media are an important approach for future agile applications. The most widely studied configurations are cross-phase modulation wavelength converters (XPM-WC) [2] and cross-gain modulation wavelength converters (XGM-WC) [3]. Both configurations require two input optical signals, one carrying the input data on an original wavelength and the other a CW probe at the new wavelength generated by a local laser, as shown in Fig. 1(a) and (b). The CW probe is supplied by a separate laser and must tune to a new wavelength within nanoseconds [1] for agile applications. XGM-WC in semiconductor optical amplifiers (SOAs) is the most widely studied due to its simplicity. The SOA gain is modulated through carrier depletion by an information-carrying signal presented to its input at the wavelength λ_s and typically occurs at input signal powers of about -10 dBm. Although the simplicity of an XGM-WC

Manuscript received June 06, 2001; revised December 04, 2001. This work was supported in part by DARPA under NGI grant MDA972-99-1-006, the DARPA-sponsored MOST Center, the State of California under Microgrant N 99-009, and New Focus Corporation.

The authors are with the Optical Communications and Photonic Networks Group, Department of Electrical and Computer Engineering, University of California—Santa Barbara, Santa Barbara, CA 93106 USA (e-mail: olavrova@engineering.ucsb.edu).

Publisher Item Identifier S 0733-8724(02)03334-0.

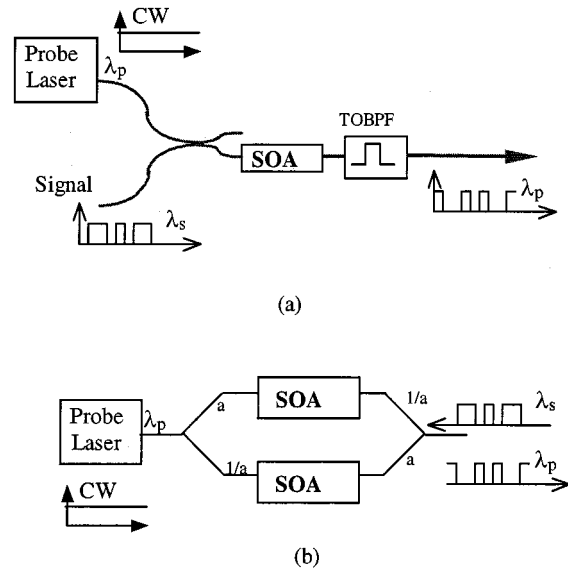


Fig. 1. Schematic of (a) XGM-WC and (b) XPM-WC and the associated local tunable laser.

is an advantage, the extinction ratio (ER) is degraded an unequal amount for up-frequency and down-frequency conversion and the SNR is degraded due to amplified spontaneous emission (ASE). XPM-WCs that employ SOAs rely on the modulation of the refractive index in the active region by the input signal, and this phase modulation can be converted to intensity modulation through the use of an interferometer or an optical bandpass filter. Advantages of XPM-WC include ER enhancement, SNR improvement, and balanced up- and down-frequency conversion, although sensitivity to input signal average power and balancing of signal levels in multiarm interferometers is a known disadvantage. Polarization sensitivity is a critical issue that can be successfully addressed in XGM-WCs through design of the gain medium and waveguide, although sensitivity of the XPM-WC is more difficult to address due to the need to maintain polarization state over a more complex integrated waveguide structure that may incorporate both active and passive semiconductor waveguides. Two-stage SOA-based converters that employ XGM followed by XPM can solve many of these problems address many of these issues by converting an arbitrary polarization signal to an internal wavelength and then to the final wavelength.

In this paper, we demonstrate that a widely tunable laser can be used as a rapidly tunable wavelength converter using gain-suppression WC technique. Wavelength conversion at 10 Gb/s to one wavelength at a time was demonstrated using a

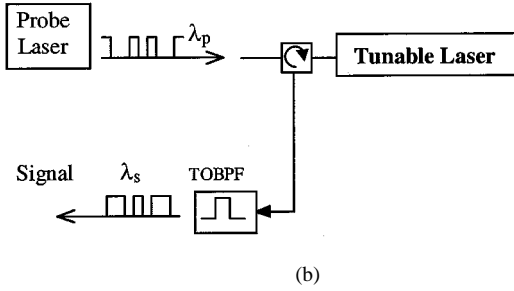
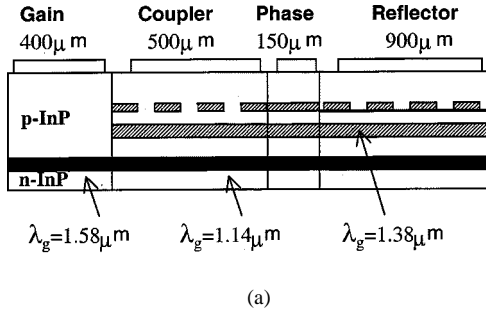


Fig. 2. (a) Schematic of a widely tunable GCSR laser and (b) wavelength conversion using gain suppression in a tunable laser.

superstructure-grating distributed Bragg reflector (SSG-DBR) laser [4], with WC to one wavelength at a time and output extinction ratios on the order of 5 to 10 dB over a 30-nm tuning window. We demonstrate dynamic conversion of any wavelength to any wavelength across 30-nm using a single grating assisted coupler sampled reflector (GCSR) laser with much higher ER values than previously reported. The output wavelength is set by rapidly changing the current in one of the laser sections. Wavelength conversion, in this case, is achieved through the gain suppression of the lasing mode by the injected signal light (probe).

II. MULTISECTION LASER WC

The schematic picture of the GCSR laser is shown in Fig. 2(a). The laser consists of four sections: a gain section followed by a grating assisted codirectional coupler section, a phase tuning section, and then a reflector section with a sampled DBR (S-DBR) mirror. By adjusting the current through the coupler section, it is possible to select lasing on one of the reflection peaks of the sampled Bragg grating. The wavelength of the selected Bragg peak and the exact mode position can thereafter be controlled like that for a conventional DBR laser, i.e., by current injection into the Bragg section and phase section, respectively. Hence, a wide continuous tuning range can be achieved by using all three tuning currents. Device fabrication, tuning mechanisms, and performance of these lasers have been described elsewhere [5], [6]. GCSR lasers can be made to operate at any of the wavelengths within the tuning range by proper setting of the coupler, reflector, and phase sections' currents. Lasing can be tuned to any wavelength within the tuning range with ± 1 GHz accuracy; the widest GCSR tuning range reported so far is 114 nm [5].

Wavelength conversion through gain suppression is a less studied WC technology than XPM or XGM and can be realized

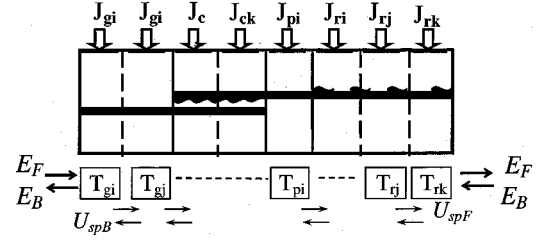


Fig. 3. Illustration of TMM.

using widely tunable single-mode semiconductor lasers such as that illustrated in Fig. 2(b). The lasing mode intensity of the laser is modulated by the input probe light and the data carried by the input probe wavelength is converted to that of the lasing mode. Among the most important advantages of this technique are the modulation format transparency, tunability of the converted signal wavelength, high conversion efficiency, and extinction ratio and single element simplicity. There are several potential disadvantages with semiconductor laser converters, namely: 1) no conversion to equal wavelength; 2) polarization sensitivity; and 3) requirement of high-input signal intensity. However, there are solutions to overcoming these problems. For example, arbitrary input signal wavelength can be converted to arbitrary wavelength, including the same wavelength, by utilizing a cascaded semiconductor laser converters configuration [1].

III. NUMERICAL SIMULATION RESULTS

Numerical simulations of wavelength conversion in a GCSR laser were carried out using a model described in detail in [6]. This model combined transfer matrix method (TMM) techniques with multimode rate equations in order to take into account spatially and temporally varying physical processes in the laser cavity such as longitudinal mode spatial hole burning (SHB), complex grating structures, nonlinear gain compression, and refractive index changes with carrier injection. The basis of the TMM is to divide each laser section longitudinally into a number of arbitrarily small elements where the structural and material parameters are assumed to be homogeneous throughout each element as shown in Fig. 3. Each element is characterized by its own 2×2 complex transfer matrix that modifies the forward and backward travelling wave amplitudes (TWAs) as they propagate through the section. By calculating TWAs of the electric field and solving the multimode photon rate equation, we can solve for transient and steady-state characteristics of the laser.

For the case of wavelength conversion with an external optical injection, well-known rate equations have to be modified as follows [4], [7]:

$$\begin{aligned} \frac{dS_{\text{out}}}{dt} &= -\frac{S_{\text{out}}}{\tau_p} \\ &\quad + v_g \Gamma \frac{dg}{dN} (1 - \varepsilon S_{\text{out}} - 2\varepsilon S_{\text{in}}) (N - N_0) S_{\text{out}} \\ \frac{dN}{dt} &= \eta_i \frac{I}{eV} - \frac{N}{\tau_s} + v_g \frac{dg}{dN} \\ &\quad \cdot (1 - \varepsilon S_{\text{out}} - 2\varepsilon S_{\text{in}}) (N - N_0) S_{\text{out}} \\ &\quad + v_g \frac{dg}{dN} (1 - \varepsilon S - 2\varepsilon S_{\text{in}}) (N - N_0) S_{\text{in}} \end{aligned}$$

TABLE I
PARAMETERS USED IN SIMULATION

Parameter	Unit	Value
Gain section length, L_g	μm	500
Waveguide thickness, d	μm	0.2
Waveguide width, w	μm	1.5
Active section waveguide loss, α	cm^{-1}	40
Active section group index, n_g	-	4
Gain compression parameter, ϵ	cm^{-3}	1.5×10^{-17}
Transparency carrier density, N_{tr}	cm^{-3}	1.15×10^{18}
Differential gain, dg/dN	cm^2	2×10^{-16}
Coupler section length, L_c	μm	500
Coupler center wavelength at zero bias, λ_c	μm	1.605
Tuning efficiency, dn/dN	cm^{-3}	-17×10^{-21}
Reflector section length, L_r	μm	900
Reflector center wavelength at zero bias, λ_r	μm	1.605
Phase section length, L_p	μm	150
Non-radiative recombination coeff., A	s^{-1}	0.5×10^8
Radiative recombination coeff., B	$\text{cm}^3 \text{s}^{-1}$	1×10^{-10}
Auger recombination coeff., C	$\text{cm}^6 \text{s}^{-1}$	2.5×10^{-29}

where N , τ_p , τ_s , v_g , Γ , dg/dN , I , e , V , ϵ , and S_{in} are the carrier density in the waveguide, photon lifetime, carrier lifetime, group velocity, optical confinement factor, differential gain coefficient, bias current, electric charge, volume of the waveguide, gain compression coefficient, and the input (probe) photon density, correspondingly. Typical values for these and other parameters used in the simulation, as well as other simulation details (including the issues of how to include noise and multimode conditions in these equations), are shown in Table I and are described in more detail in [6].

A high-output ER and open eye pattern are among the most important criteria for digital wavelength conversion. In order to determine the operating currents that optimize these parameters, we have performed simulations at different gain section bias currents. The calculated ER as a function of gain section current for different wavelengths is shown in Fig. 4 (signal bit rate of 10 Gb/s for a probe-signal intensity of 10 mW and an ER of 35 dB). The ER of the converted signal is highest for gain currents just above the threshold and decreases with further increase of the gain section current. Also, this curve stays true for a large number of different output wavelengths throughout the tuning range of the GCSR laser.

Typical calculated eye diagrams for $I = 0.95 \cdot I_{th}$, $I = 1.0 \cdot I_{th}$, $I = 1.1 \cdot I_{th}$, and $I = 5 \cdot I_{th}$ are shown in Fig. 5(a)–(d), respectively, at a signal bit rate of 10 Gb/s for a probe-signal intensity of 10 mW. From these figures, a clear eye opening is observed for the case of $I = 1.1 \cdot I_{th}$, whereas the situation degrades for $I = 1.0 \cdot I_{th}$ or $I = 5 \cdot I_{th}$ cases. This is due to the fact that, at currents much higher than the threshold, the GCSR gain is too strong to be suppressed by the intensity of the probe signal. On the other hand, with currents equal to the threshold or smaller, there is not enough gain in the structure and the noise effects are too strong to create a good eye opening. Thus, $I = 1.1 \cdot I_{th}$ was chosen as our operation point for the experiment described further in this paper.

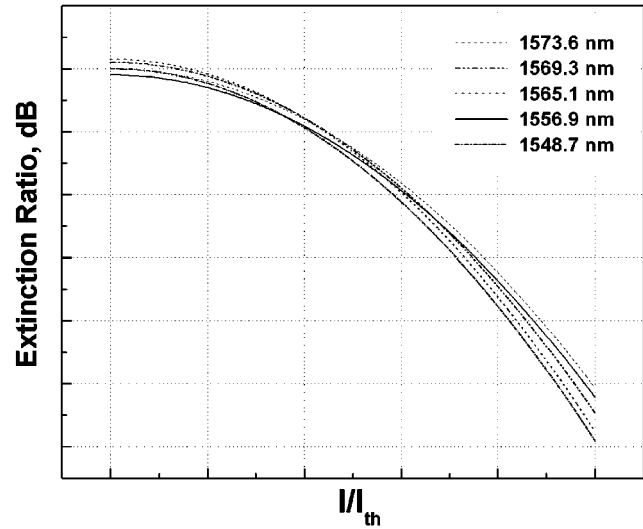


Fig. 4. Calculated ER for as a function of gain section current for different wavelengths.

IV. EXPERIMENTAL RESULTS

A schematic of the experiment is shown in Fig. 6. A tunable CW light source (probe) and electrooptic modulator (EOM) were used to generate the 10-Gb/s signal that was launched into the gain section of the GCSR laser using a circulator and an antireflection (AR)-coated lensed fiber. An optical filter was used to filter out the noise after the EFDA that was used to boost the power of the CW laser. The output signal was collected at the other port of the circulator using an optical filter (with a 0.8-nm bandwidth) tuned to the output wavelength and analyzed with OSA, BERT, and digital oscilloscope.

First, we demonstrated wavelength conversion between different input pump wavelengths and different output wavelengths and measured the ER of the converted signal. Fig. 7 shows a

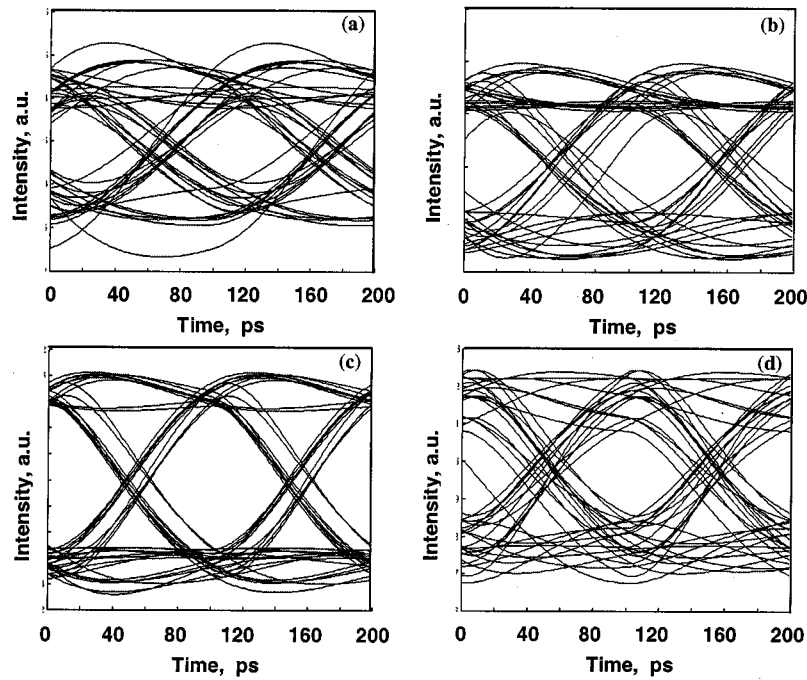


Fig. 5. Optical output waveforms (at the output wavelength) for gain section currents (a) $I = 0.95 \cdot I_{th}$, (b) $I = 1.0 \cdot I_{th}$, (c) $I = 1.1 \cdot I_{th}$, and (d) $I = 5 \cdot I_{th}$. Input pump power 10 mW.

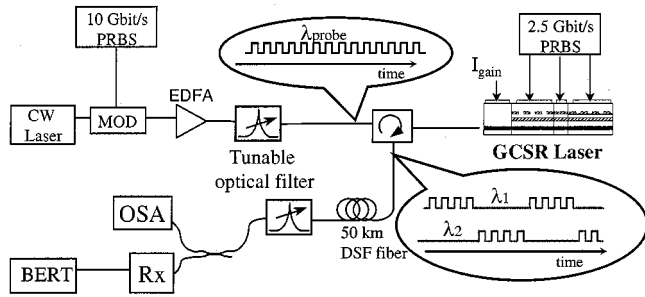


Fig. 6. Schematic of the experimental setup. MOD: external modulator; EDFA: erbium-doped fiber amplifier; OSA: optical spectrum analyzer; Rx: receiver; BERT: bit error rate tester; PRBS: pseudorandom binary sequence.

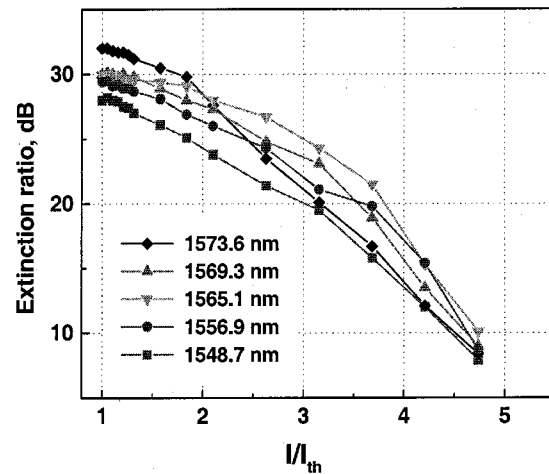


Fig. 8. ER of the converted wavelength signal as a function of the gain section current.

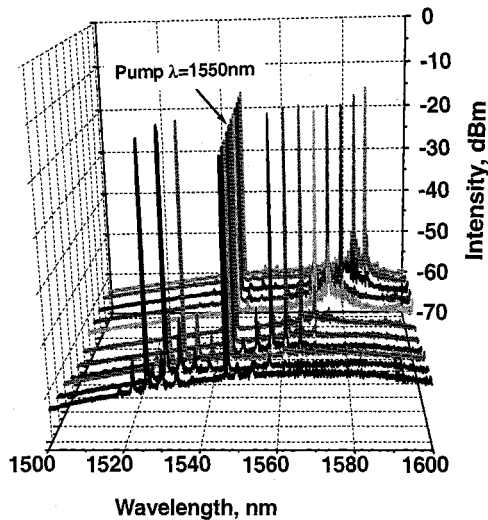


Fig. 7. Time-averaged WC spectra for wavelength conversion between a fixed pump wavelength ($\lambda = 1550$ nm) and different output wavelengths.

time-averaged optical spectra for different output wavelengths and a fixed pump wavelength $\lambda = 1550$ nm at a signal rate of 10 Gb/s. Similar curves can be obtained for other pump wavelengths. A high side mode suppression ratio (~ 30 dB) was observed for all converted outputs.

Fig. 8 shows the measured ER as a function of the gain section current for different lasing wavelengths. As predicted by the simulation, the ER is higher at gain section currents around the threshold and decreases at higher currents. However, at currents around threshold, the output power of the GCSR laser is not very high (on the order of -20 dBm), but it increases with higher gain currents. Thus, the operation point should be set at a point that optimizes both the ER (currents just above the threshold) and output power (currents much higher than the threshold). There is only a small difference in the calculated values of ER (Fig. 4)

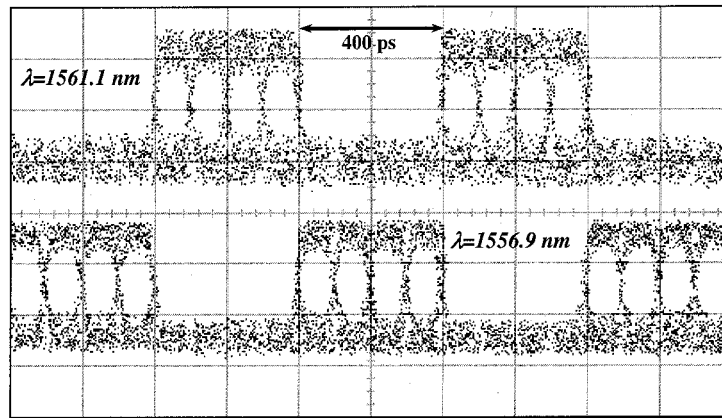


Fig. 9. Real-time switching of 10-Gb/s data between $\lambda = 1561.1$ nm and $\lambda = 1556.9$ nm.

and experimentally measured ones (Fig. 8); this is due to the idealized pump signal quality used in the simulation.

Next, we performed wavelength conversion at 10 Gb/s while switching the output wavelength at a 2.5-GHz switching rate. Each bit at 10 Gb/s is converted from the probe wavelength ($\lambda = 1550$ nm) to the output wavelength, while the output wavelength is changed between different λ 's every fourth bit. For example, Fig. 9 shows switching between $\lambda = 1561.1$ nm and $\lambda = 1556.9$ nm waveforms. These waveforms were taken by tuning the output optical filter to a corresponding wavelength. The fundamental limitation on the wavelength switching speed of the present scheme is the carrier density dynamics (carrier density injection and recombination times) in the tuning sections of the GCSR laser. With a proper laser structure design, wavelength switching time can be optimized to be faster than 2.5 Gb/s. However, 2.5-Gb/s switching speed is good enough for such photonics applications as all-optical label swapping and wavelength routing [1] where the wavelength determines the label of the packet and the data is encoded at a higher speeds within the packet payload.

The converted data was then propagated over a distance of 50 km of dispersion shifted fiber and the BER was measured. The GCSR gain section current was maintained at $I = 1.1 \cdot I_{th}$ and input pump power at 10 dBm. Fig. 10 shows back-to-back, WC, and WC + 50 km transmission BER measurements for different output wavelengths. No BER floors were observed. A power penalty of 2 dB is observed due to the WC, and a power penalty of approximately 2.5 dB is observed due to transmission effects. A small power penalty variation of approximately 0.5 dB is observed for transmission at different wavelengths, which shows a good uniformity of WC throughout the tuning range.

V. SUMMARY AND CONCLUSION

We have demonstrated that a widely tunable laser can be used as a rapidly tunable wavelength converter using gain-suppression WC technique and performed high-bit-rate WC with simultaneous switching of the output wavelength. High ER (> 25 dBm) and small power penalty over 30-nm wavelength range were observed. Successful transmission of the converted signal over 50 km of DSF fiber was demonstrated with a power penalty

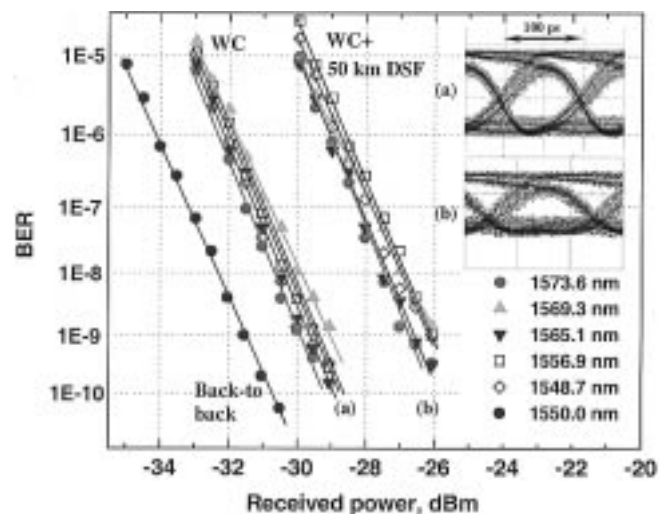


Fig. 10. BER measurements for transmission over 50 km of DSF for different wavelengths (pump $\lambda = 1550$ nm). The inset shows eye diagrams for (a) the WC only and (b) WC + 50 km of DSF cases.

of only 2.5 dB. WC polarization sensitivity is an important issue and will be studied in future work.

ACKNOWLEDGMENT

The authors would like to thank ADC for providing the GCSR laser chips.

REFERENCES

- [1] D. J. Blumenthal, B.-E. Olsson, G. Rossi, T. E. Dimmick, L. Rau, M. Masanovic, O. Lavrova, R. Doshi, O. Jerphagnon, J. E. Bowers, V. Kaman, L. A. Coldren, and J. Barton, "All-optical label swapping networks and technologies," *J. Lightwave Technol.*, vol. 18, pp. 2058–2075, Dec. 2000.
- [2] B. E. Olsson *et al.*, "A simple and robust 40-Gb/s wavelength converter using fiber cross-phase modulation and optical filtering," *IEEE Photon. Technol. Lett.*, vol. 12, pp. 846–848, July 2000.
- [3] P. Ohlen, B. E. Olsson, and D. Blumenthal, *Proc. Conf. Lasers Electro-Optics*, 2000, pp. 279–280.
- [4] H. Yasaka, H. Sanjoh, H. Ishii, Y. Yoshikuni, and K. Oe, *J. Lightwave Technol.*, vol. 15, pp. 334–341, Feb. 1997.
- [5] P.-J. Rigole, S. Nilsson, L. Backbom, T. Klinga, J. Wallin, B. Stalnacke, E. Berglind, and B. Stoltz, "114-nm wavelength tuning range of a vertical grating assisted co-directional coupler laser with a super structure grating distributed Bragg reflector," *IEEE Photon. Technol. Lett.*, vol. 7, pp. 697–699, July 1995.

- [6] O. Lavrova and D. J. Blumenthal, "Detailed transfer matrix based dynamic model for multisection widely-tunable GCSR lasers," *J. Lightwave Technol.*, vol. 18, pp. 1274–1283, Sept. 2000.
- [7] L. A. Coldren and S. Corzine, *Semiconductor Lasers and Photonic Integrated Circuits*. New York: Wiley, 1995.



Olga A. Lavrova was born in St. Petersburg, Russia, in 1974. She received the B.S. degree in physics and the M.S. degree in electrical engineering from the St. Petersburg State Electrical Engineering University, St. Petersburg, and the Ph.D. degree from the Electrical and Computer Engineering Department of the University of California—Santa Barbara, Santa Barbara, in 2001.

Her work includes experimental and analytical studies of widely tunable semiconductor lasers and their applications in wavelength agile optical

network systems.



Lavanya Rau (S'99) received the Master's degree in physics from the Indian Institute of Technology, Bombay, in August 1995. She is currently pursuing the Ph.D. degree in optical communication at the University of California—Santa Barbara, Santa Barbara.

In 1997, she worked at the Lawrence Livermore National Laboratory, where she studied the effectiveness of acoustooptic tunable filter (AOTF) in the National Transparent Optical Network Consortium (NTONC) network. Her research interests include optical wavelength conversion, optical subcarrier

multiplexing, and optical internet protocol routing.



Daniel J. Blumenthal (S'91–M'93–SM'97) received the B.S.E.E. degree from the University of Rochester, Rochester, New York, in 1981, the M.S.E.E. degree from Columbia University, New York, in 1988, and the Ph.D. degree from the University of Colorado, Boulder, in 1993.

In 1981, he worked at StorageTek, Louisville, CO, in the area of optical data storage. In 1986, he worked at Columbia University in the areas of photonic switching systems and ultrafast all-optical networks and signal processing. From 1993 to 1997, he was

Assistant Professor in the School of Electrical and Computer Engineering, Georgia Institute of Technology, Atlanta. He is currently the Associate Director for the Center on Multidisciplinary Optical Switching Technology (MOST) and a Professor of Electrical and Computer Engineering at the University of California, Santa Barbara. He is the cofounder of Calient Networks, San Jose, CA, a microelectromechanical systems-based photonic switch manufacturer. His current research areas are in optical communications, WDM, photonic packet switched and all-optical networks, all-optical wavelength conversion, optical subcarrier multiplexing, and multispectral optical information processing. He has authored or coauthored more than 100 papers in these and related areas. He has served as an Associate Editor for IEEE PHOTONICS TECHNOLOGY LETTERS and IEEE TRANSACTIONS ON COMMUNICATIONS. He was a Guest Editor for the JOURNAL OF LIGHTWAVE TECHNOLOGY Special Issue in Photonic Packet Switching Systems, Technologies, and Techniques published in December 1998. He also served as the General Program Chair for the 2001 OSA Topical Meeting on Photonics in Switching and as Program Chair for the 1999 OSA Topical Meeting on Photonics in Switching. He has served on numerous other technical program committees, including the Conference on Optical Fiber Communications (OFC) in 1997, 1998, 1999, and 2000, and the Conference on Lasers and Electrooptics (CLEO) in 1999 and 2000.

Dr. Blumenthal is a member of the Optical Society of America (OSA) and the IEEE Lasers and Electro-Optics Society (LEOS). He received a 1999 Presidential Early Career Award for Scientists and Engineers (PECASE) from the White House and the Department of Defense, a 1994 NSF Young Investigator (NYI) Award, and a 1997 Office of Naval Research Young Investigator Program (YIP) Award.